Journal of Alloys and Compounds, 189 (1992) 9–15
JALCOM 356

Crystallographic properties of $Ce(Si,Ge)_{2-x}$ solid solutions

N. Boutarek and R. Madar
Institut National Polytechnique de Grenoble, E.N.S.P.G., BP 46, 38402 St. Martin d'Hères (France)

B. Lambert-Andron
Laboratoire de Cristallographie, C.N.R.S., 166X, 38042 Grenoble (France)

S. Auffret and J. Pierre
Laboratoire L. Néel, C.N.R.S., 166X, 38042 Grenoble (France)

(Received February 10, 1992)

Abstract

Some crystallographic properties of solid solutions of the Ce–Si–Ge system were investigated. A new type of superstructure was observed in the compound $CeGe_{0.66}Si_{0.92}$, with an alternation of silicon- or germanium-rich planes; this compound undergoes a crystallographic transition at low temperature. Two different tetragonal phases coexist at room temperature for the compound $CeGe_{1.2}Si_{0.475}$. These observations are related to phase transformations previously observed in silicides and to the frequent ordering of vacancies in the lattice of rare earth silicides and germanides.

1. Introduction

Numerous studies have been devoted to the determination of the crystal structure and physical properties of cerium silicides and germanides with formulae close to CeX_2 [1–3]. In particular, the properties of $CeSi_{2-x}$ have been widely studied in relation to the occurrence of Kondo behaviour or intermediate valence states [4–6]. More recently, several studies have been undertaken on $CeGe_xSi_{2-x}$ solutions, where hybridization between the 4f electron and the conduction band varies with silicon content [7, 8]. These compounds crystallize in two main structural types, namely $ThSi_2$ ($I4_1/amd$) and orthorhombic $GdSi_{2-x}$ (*Imma*), depending on the composition. A curious feature is the transition of $CeSi_{2-x}$ compounds from tetragonal to orthorhombic on lowering the silicon concentration, whereas the reverse is observed in $CeGe_{2-x}$ on lowering the germanium concentration.

Various types of superstructure have been observed in rare earth (RE) silicides and germanides, and related to the ordering of vacancies. Electron microscopy has revealed extra spots in the (a^*, a^*) plane in one low-temperature phase of $CeSi_{1.86}$ [9]. $CeGe_{1.6}$ exhibits a ($3a$,$3a$) superstructure [10], with a succession of dense and vacant planes of germanium along the c axis. Orthorhombic phases of rare earth silicides $RESi_{2-x}$ show a selective repartition of vacancies on one of the two silicon sites of the $GdSi_{2-x}$ structure [11, 12], again giving an alternation of more or less dense silicon planes along the c axis.

In this paper, the crystallographic structure and certain transport properties of several Ce–Ge–Si ternary compounds are investigated. A part of the ternary phase diagram is drawn in Fig. 1, showing the location of the samples studied.

The first aim was to study solid solutions between tetragonal $CeSi_{1.9}$ and tetragonal $CeGe_{1.6}$, in an attempt to retain the $ThSi_2$ structure, and focusing on the ordering of silicon, germanium and vacancies in the structure. The second aim was to obtain new information on magnetic and transport properties as a function of hybridization in the series. These latter properties will be described in detail in a following paper.

2. Preparation of the samples

Polycrystalline bulk samples of varying composition $Ce(Ge_{1.6})_x(Si_{1.9})_{1-x}$ with $x=0$, 0.15, 0.25, 0.5, 0.75, 0.85 and 1 were prepared. Corresponding mixtures of cerium rods (purity, 99.9%) and silicon and germanium lumps (purity, 99.9999%) were melted using the inductive method in a cooled copper Hukin-type crucible in argon. The powdered samples for X-ray investigations were

0925-8388/92/$5.00

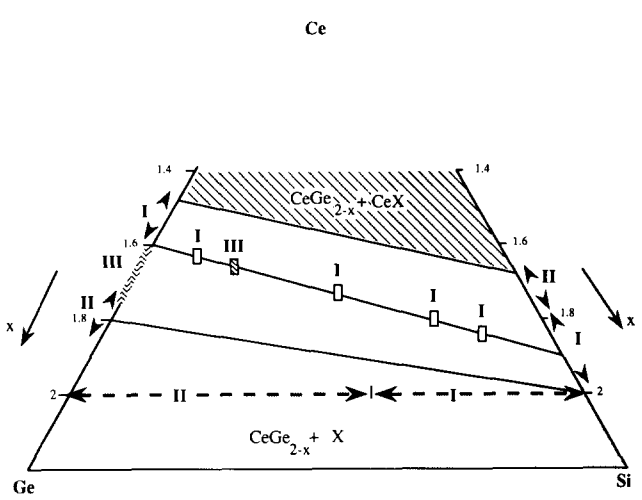

Fig. 1. Tentative phase diagram in the Ce–Ge–Si system near the CeX_2 composition (after refs. 1, 2, 3, 8 and 13 and the present work): I, monophase domain, tetragonal $ThSi_2$ type; II, monophase domain, orthorhombic $GdSi_2$ type; III, biphase domain (two tetragonal cells, $ThSi_2$ type); – – –, measured line by Mayer and Eshdat [1]; □, experimental points of the $CeSi_{1.9}$–$CeGe_{1.6}$ solution.

ground in an argon atmosphere and annealed for 48 h at 800 °C in high vacuum.

A large single crystal was grown, starting from a $CeGe_{0.8}Si_{0.95}$ polycrystalline alloy, by a modified Czochralski technique described elsewhere [14]; the crystal was pulled from the induction-levitated melt, while the polycrystalline rod of the alloy was pushed simultaneously inside the cold crucible. The pulling rate was 3 mm h^{-1} and [100] was found to be the preferred growth direction.

The chemical composition of the single crystal was $CeGe_{0.66}Si_{0.92}$, as determined by microprobe analysis. The smaller amount of germanium in the single crystal compared with the initial composition of the starting alloy can probably be explained by the evaporation of germanium during crystal growth.

The density of the crystal, measured using Archimedes' method with CCl_4 as immersion liquid, was found to be $d_m = 5.88 \pm 0.05$ g cm^{-3}. This value is higher than that calculated from the previous formula ($d_c = 5.76$ g cm^{-3}), and corresponds to about $CeGe_{0.72}Si_{0.92}$, assuming the same silicon content.

The single-crystal rod was oriented by X-ray Laue diffraction. A small crystal was used for crystallographic studies, and slices measuring 6 mm × 1 mm × 0.7 mm were cut along the [100] and [001] crystallographic axes for magnetization and resistivity measurements.

3. Structural investigations

At room temperature, $CeSi_{2-x}$ compounds with $x < 0.20$ crystallize in the tetragonal-type structure $ThSi_2$ with space group $I4_1/amd$. An increase in x initially leads to the creation of silicon vacancies without modification of the symmetry. For $x > 0.20$ the compounds crystallize in the orthorhombic $GdSi_{2-x}$ structure (space group *Imma*). The limit of the homogeneity range is estimated to be $x = 0.4$.

A crystallographic phase transformation has recently been observed in the tetragonal phase $CeSi_{1.86}$ [9], leading, near 200 K, to a phase separation into two nearly tetragonal phases which coexist at lower temperatures. This phase transformation shows some thermal hysteresis, and the two phases have different cell volumes (relative difference of about 1.4% at 4.2 K). Electron microscopy has revealed that a superstructure occurs in at least one of the phases, probably related to the ordering of vacancies on the silicon site.

This phenomenon also occurs in the tetragonal phase of $PrSi_{1.9}$, [15], and has also recently been observed for $LaSi_{1.9}$. Thus the tetragonal $ThSi_2$ form may undergo a phase transformation, either when the silicon content is lowered, or when the temperature is lowered (as already known for heavier rare earth compounds from neodymium to dysprosium).

Conversely, $CeGe_{2-x}$ with a cerium to germanium ratio close to 1:2 crystallizes in the $GdSi_{2-x}$ orthorhombic structure type [1]; the creation of vacancies in the germanium sublattice leads to the appearance of a tetragonal structure. For a composition close to $CeGe_{1.6}$ the vacancies are ordered in a superstructure of $ThSi_2$: $a = 3a_t$, $c = c_t$, with the space group $I4_1$ [10], where a_t and c_t are the lattice parameters of the original $ThSi_2$ structure.

3.1. Variations in the lattice constants in $Ce(Ge_{1.6})_x(Si_{1.9})_{1-x}$ solutions

The room-temperature lattice parameters of the samples were determined by X-ray powder diffraction in a Seeman–Bohling-type focusing camera, using Cr $K\alpha_1$ radiation with silicon as internal calibration standard.

The analysis of the X-ray diffraction data shows that the diffraction pattern of the compounds studied can be indexed with the $ThSi_2$ structure. The orthorhombic $GdSi_2$ structure type, reported by Mayer and Eshdat [1] in $CeGe_xSi_{2-x}$ solutions with $x > 1.2$, has not been observed.

By substituting silicon with germanium up to $y = 0.5$, germanium atoms replace the silicon in the lattice at random and the tetragonal structure remains unchanged. However, in the compounds rich in germanium ($x > 0.5$) weak lines are observed in the diffraction diagram providing evidence of ordering effects and superstructures. In a first step, these additional reflections were neglected and the lattice parameters were calculated assuming the tetragonal $ThSi_2$ cell.

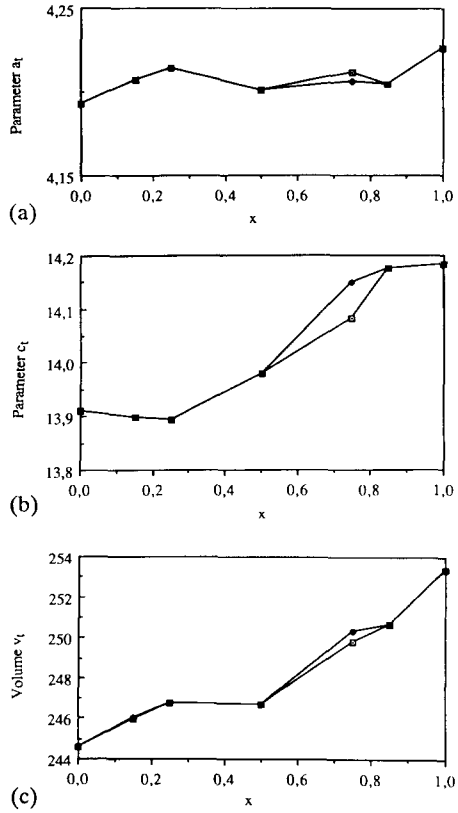

Fig. 2. Variation in the lattice parameters and cell volume of $Ce(Ge_{1.6})_x(Si_{1.9})_{1-x}$ solutions *vs.* composition at room temperature.

A part of the $CeGe_{0.66}Si_{0.92}$ single crystal was crushed to powder and diffraction patterns were obtained using a focusing camera. Reflection peaks at room temperature can be indexed in a tetragonal cell with $a_t = 4.200(2)$ Å and $c_t = 13.979(2)$ Å, and are related to the $ThSi_2$ structure. No extra lines are observed.

For comparison, the $CeSi_{1.9}$ cell parameters are $a_t = 4.191$ Å and $c_t = 13.899$ Å at room temperature [9], whereas those for $CeGe_{1.6}$ are $a = 12.680$ Å $= 3a_t$ and $c_t = 14.184$ Å [10].

The $CeGe_{1.2}Si_{0.475}$ powdered sample contains two phases; the strong lines in the diffraction pattern can be indexed in two different tetragonal $ThSi_2$ structures, with the lattice constants: $a_t = 4.201(2)$ Å and $c_t = 14.149(2)$ Å and $a_t = 4.217(2)$ Å and $c_t = 14.083(2)$ Å. This situation is thus similar to that of $CeSi_{1.86}$ at low temperatures, where a phase separation occurs at about 200 K [9]. The variations in the room-temperature lattice constants for the solid structures are shown in Fig. 2.

3.2. Low-temperature diffraction and phase transitions in $CeGe_{0.66}Si_{0.92}$

An analysis of the resistivity measurements for $CeGe_{0.66}Si_{0.92}$ single crystals (see below) indicates that a phase transition occurs at low temperature. To obtain a better understanding of this anomalous resistivity behaviour, we studied the thermal expansion of $CeGe_{0.66}Si_{0.92}$.

The thermal expansion studies were carried out on the crystal using X-ray diffraction in the θ–2θ geometry with Fe $K\alpha_1$ radiation. X-ray data were collected in the temperature range 12–300 K; the diffraction planes were (h00) and (00l). The values for the tetragonal lattice parameters were obtained from the Bragg angles of (4 0 0) and (0 0 12) reflections. Measurements were carried out with decreasing and increasing temperature in order to determine the occurrence of phase transitions.

Figures 3(a) and 3(b) show the temperature dependence of the a_t and c_t lattice parameters. During cooling or heating cycles, parameter a_t shows a regular variation. Its value increases with increasing temperature; however, hysteresis is observed between 150 and 200 K, in agreement with resistivity data. During initial cooling, parameter c_t exhibits a strong anomaly at temperatures below 50 K. This discontinuity obviously has a crystallographic origin, as no magnetic order occurs down to 9 K as shown by magnetic susceptibility measurements. During heating, no anomaly occurs near 50 K, but a large anomalous thermal expansion is observed between 150 and 200 K, with a change in the temperature slope. The value of the parameter above 200 K exceeds that of the virgin sample, showing that the starting crystallographic state has not yet been recovered.

All of these results are in agreement with resistivity data, and show the occurrence of a strong hysteresis in the crystallographic transformation.

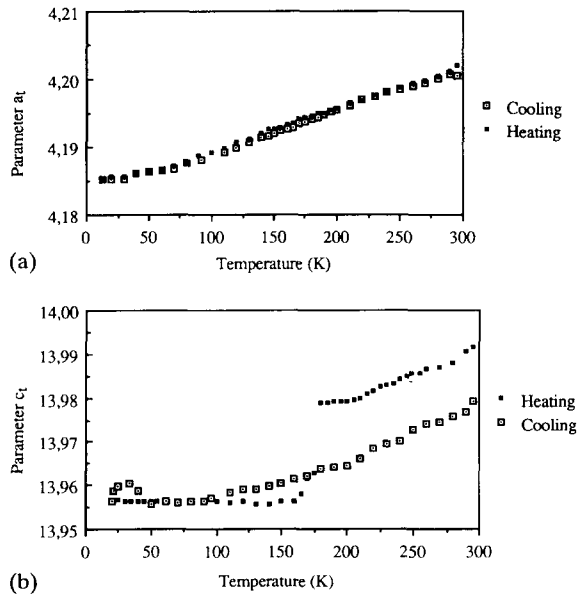

Fig. 3. Thermal variation in the lattice parameters a_t and c_t of the $CeGe_{0.66}Si_{0.92}$ single crystal.

3.3. Superstructure of $CeGe_{0.66}Si_{0.92}$

X-ray diffraction experiments were performed at room temperature on a virgin single crystal using a four-circle diffractometer. The experimental conditions are given in Table 1. The reflections were collected and indexed in the tetragonal cell $a=4.198(2)$ Å and $c=14.004(2)$ Å, in fair agreement with the powder data obtained with the focusing camera.

The diffraction selection rule $h+k+l=2n$ is observed, but not the condition $2k+l=2n+1$ or $4n$ corresponding to the 4a and 8e positions of the $ThSi_2$ structure. The crystal shape was approximated to a sphere of radius $r\approx 0.1$ mm. An examination of the equivalence of the diffracted intensities shows that the true symmetry is not tetragonal, but orthorhombic. The new cell is $a=-a_t+b_t=5.937$ Å; $b=c_t=14.004$ Å; $c=a_t+b_t=5.937$ Å.

The space group was taken to be $F222$; the intensities were merged with an agreement factor of 0.035 in the Laue symmetry 222. The intensities were corrected by a spherical absorption factor, and the refinement by the least-squares method was performed using the SDP program [16]. In a first step, cerium atoms were located at the ideal positions of α-$ThSi_2$, and the positions of silicon and germanium atoms were obtained by Fourier analysis.

Twofold splitting of the 8e position of the space group $I4_1/amd$ into the two sites 8i and 8f with two different atomic scattering factors leads to symmetry reduction in the space group $F222$.

The positions and thermal parameters are given in Table 2 and the interatomic distances in Table 3. The refinement of the scattering factors for each site 8i and 8f gives the occupancy factors and a formula $CeGe_{0.66}Si_{0.95}$ in close agreement with microprobe analysis. The rather poor value of the reliability factor ($R=0.075$, $R_w=0.095$) can be related to the inaccuracy of the stoichiometry, the occurrence of some stacking faults and the approximation of a spherical shape for absorption corrections, but represents a significant improvement compared with the assumption of statistical disorder between silicon, germanium and vacancies.

TABLE 1. Experimental conditions

Diffractometer	Philips
Scan mode	θ–2θ
Scan width (deg)	1.2
Scan speed (deg s^{-1})	0.02
Limits	$3°<\theta<30°$
Number of reflections	3298
Number of independent reflections	456 ($F>4\sigma$)
Space group	$F222$
Cell dimensions (Å)	$a=5.937(2)$
	$b=14.004(2)$
	$c=5.937(2)$

The refined values of the atomic scattering factors agree with an occupation of the 8i site by silicon atoms (population, 0.95) and the 8f site by germanium (population, 0.66) and vacancies; the interatomic distances are in good agreement with this assumption: d(Si–Si)=2.12 Å, d(Ge–Ge)=2.42 Å (Table 3). The shortest Si–Si distances are much smaller than in pure silicon. This general fact which occurs in rare earth 'disilicides' is one of the major reasons for the lower silicon content of these compounds.

The cerium atoms on the 4a and 4c sites have two different environments (Fig. 4) with a succession of silicon polyhedra and germanium–vacancy polyhedra along the b axis (c axis of the $ThSi_2$ structure).

The high values of the anisotropic thermal factors (Table 2) for the sites occupied by germanium and vacancies indicate static and/or dynamic disorder; the larger displacement is found in the (a,c) plane.

4. Resistivity measurements in $CeGe_{0.66}Si_{0.92}$

Resistivity data are available for several $CeSi_{2-x}$ compounds [5, 13, 17]. For ferromagnetic phases, *i.e.* $CeSi_{1.71}$, the resistivity exhibits a Kondo-like behaviour in the paramagnetic range (nearly linear decrease as a function of the logarithm of temperature). Conversely, for silicon-rich and strongly hybridized phases ($CeSi_{2-x}$, with $x=0$–0.14), the resistivity increases with temperature.

In addition, the resistivity curves often show anomalies related to crystallographic transformations in the samples. For polycrystalline samples, Dhar *et al.* [13] have observed a progressive increase in resistivity during temperature cycles, for samples close to the magnetic–non-magnetic boundary. This has been ascribed to cracks due to the volume changes associated with the localization of Ce 4f electrons. Conversely, only a slight reproducible anomaly appears for monocrystalline $CeSi_{1.86}$ samples near 200 K due to the phase separation in this compound [19]. It should be noted that the transformation temperature hardly changes between $CeSi_{1.8}$ and $CeSi_{1.9}$.

The resistivity was measured in $CeGe_{0.66}Si_{0.92}$ on two samples from the same batch, cut along the a and c axes (of the $ThSi_2$ cell). Measurements were performed using the a.c. four-probe method; the temperature was decreased from 300 K in a virgin sample. For the current along the a axis, the resistivity is Kondo-like down to the Curie point, but decreases below the ferromagnetic Curie point $T_C=9$ K due to the suppression of spin fluctuations by magnetic order. The resistivity is reproducible during successive thermal cycles, with a faint hysteresis around 200 K.

TABLE 2. Positional and thermal parameters

Atom	X	Y	Z	$\beta(1,1)$	$\beta(2,2)$	$\beta(3,3)$	$\beta(1,3)$
Ce_1 (4a)	0.000	0.000	0.000	0.0030(2)	0.00085(4)	0.0072(3)	0
Ce_2 (4c)	0.250	0.250	0.250	0.0031(2)	0.00155(5)	0.0031(2)	0
Ge (8f)	0.000	0.5876(4)	0.000	0.019(1)	0.0010(1)	0.022(1)	0.032(2)
Si (8i)	0.250	0.8257(7)	0.250	0.0019(8)	0.0026(3)	0.004(1)	0.004(2)

The form of the anisotropic displacement parameter is: $\exp\{-(\beta(1,1)h2+\beta(2,2)k2+\beta(3,3)l2+\beta(1,2)hk+\beta(1,3)hl+\beta(2,3)kl)\}$. $\beta(1,2)=\beta(2,3)=0$.
Occupancy factors p are $p(\mathrm{Ge})=0.66(2)$ and $p(\mathrm{Si})=0.95(2)$.

TABLE 3. Interatomic distances (Å)

Atom	Distance (Å)
Ce_1–Ce_2	4.082(2)
Ce_1–Ce_1	4.198(2)
Ce_2–Ce_2	4.198(2)
Ce_1–Ge	3.212(4)
Ce_1–Si	3.219(4)
Ce_2–Ge	3.095(4)
Ce_2–Si	3.152(4)
Ge–Si	2.425(6)
Ge–Ge	2.453(6)
Si–Si	2.121(5)

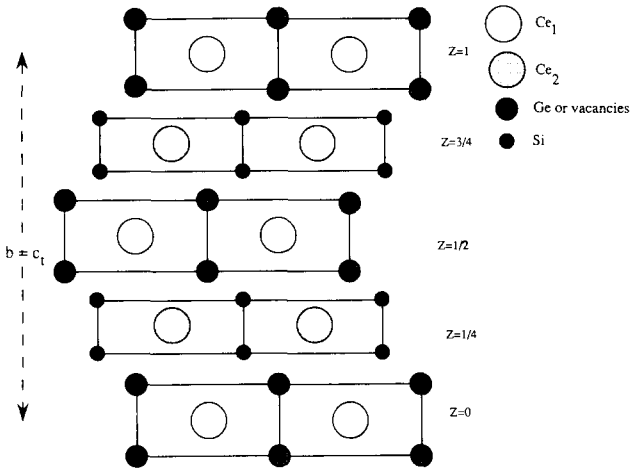

Fig. 4. Projection on the (001) plane of the orthorhombic structure of $CeGe_{0.66}Si_{0.92}$.

For the current along the c axis, the same type of behaviour is observed down to 50 K, where a sudden jump occurs in the resistivity curve (Fig. 5). The Curie temperature T_C again corresponds to a maximum in the resistivity. On increasing the temperature, rapid decreases in resistivity are observed in the temperature range 150–220 K; the initial value of the resistivity obtained for the virgin sample is not recovered, although the same negative resistivity slope is observed in the high-temperature range. Such irreversible behaviour may be attributed to the crystallographic transformation

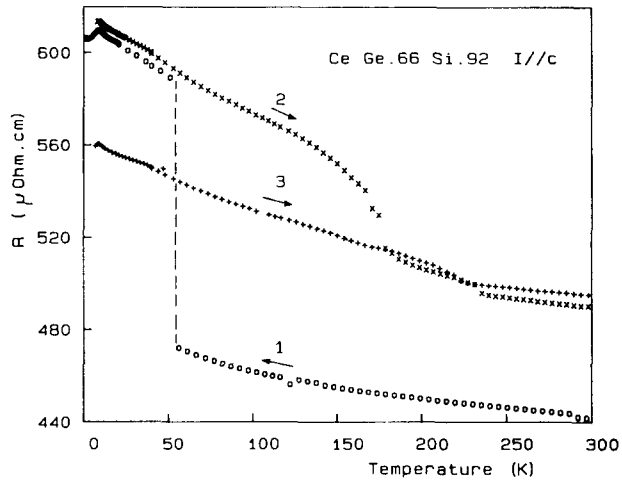

Fig. 5. Resistivity of a $CeGe_{0.66}Si_{0.92}$ single crystal along the c_t axis, during three consecutive thermal cycles. Cycle 1 is the first temperature decrease on a virgin sample and cycles 2 and 3 are two consecutive cycles with increasing temperature. The amplitude of the resistivity discontinuities progressively decreases due to the increased mixture of the crystallographic phases.

in the sample, which takes place with a large temperature hysteresis. An interesting feature is that the crystallographic transformation mainly affects the resistivity along the c_t axis.

Resistivity curves along a_t and c_t are plotted as a function of T (logarithmic scale) in Fig. 6. The resistivity curve along c_t was obtained by matching at 50 K the two parts of the curve of the first resistivity run. Despite the larger resistivity along the c_t axis (probably related to the occurrence of defects along this axis), the relative decrease in the resistivity is nearly the same along the two axes.

5. Discussion

As mentioned in Section 1, two main structural types are observed in cerium silicides and germanides, with crystallographic transformations depending on temperature and stoichiometry. Various types of superstructure are also observed.

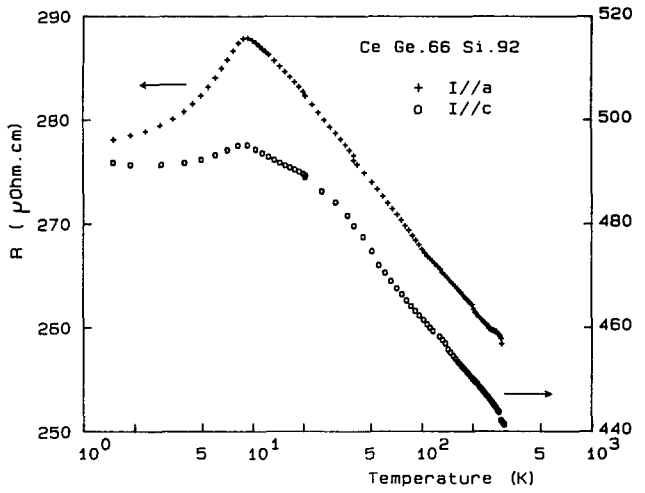

Fig. 6. Resistivity for $CeGe_{0.66}Si_{0.92}$ along a_t and c_t axes. The unique curve along c_t was obtained by matching at 50 K the data of the first temperature run.

In the case of $CeGe_{0.66}Si_{0.92}$, a new type of superstructure is observed, with an alternation of silicon- or germanium-rich planes. As in the binary $CeGe_{2-x}$ compounds, it is impossible to surround cerium by a complete germanium polyhedron, and vacancies are selectively distributed in the germanium sublattice. Moreover, the dimensions of the polyhedron surrounding one site of cerium (Ce_1 in Fig. 4) are larger than those of the polyhedron surrounding Ce_2.

Crystallographic transformations occur for many silicides as a function of temperature, *e.g.* tetragonal to orthorhombic distortions with preferential vacancy ordering on one silicon site, order–disorder transformations or phase separations in tetragonal structures. Such transformations strongly affect the resistivity. The reason for the different behaviour of the compounds, with some undergoing a simple phase transformation and others a phase separation with two coexisting phases at low temperature, is not clear at present. Two relevant parameters may be the transformation temperature via the activation energy and the density of vacancies.

Good concordance is obtained for $CeGe_{0.66}Si_{0.92}$ between the temperature of anomalies observed by crystallographic and resistivity methods. On lowering the temperature for a virgin sample, the resistivity shows an anomaly at 50 K with the current along the *b* axis (c_t axis of the $ThSi_2$ structure), and an anomaly of the variation in the lattice parameter is observed at the same temperature. Similarly, increasing temperature leads to lattice parameter and resistivity anomalies near 180 K.

These crystallographic transformations may be attributed to rearrangements in the lattice, which probably affect mainly the repartition of vacancies on the germanium sublattice as discussed above. The anomalies are mainly observed along the *b* axis (c_t axis of $ThSi_2$), which means that stacking faults should occur mainly along this axis in agreement with the description of the structure.

Finally, the ternary Ce–Ge–Si phase diagram for the considered stoichiometry is not simple. A transformation from the tetragonal to orthorhombic phase is observed on lowering the silicon content, whereas the opposite occurs for germanides. It seems, from the present study, that two different tetragonal (or slightly distorted) structures may appear in these systems, corresponding to different cerium to X ratios, *e.g.* in the $CeGe_{1.2}Si_{0.475}$ compound two different tetragonal structures coexist at room temperature. However, at the present time we have not been able to determine a difference in the composition of these two phases. In addition, the pseudo-tetragonal symmetry deduced from the value of the lattice parameters may mask a lower symmetry in the distribution of silicon, germanium and vacancies.

In future investigations, a neutron diffraction experiment will be performed on a single crystal in order to determine precisely the evolution of the structure with increasing or decreasing temperature, since the neutron scattering lengths for silicon and germanium are more favourable than those occurring in X-ray diffraction. In addition, the magnetic structure will be studied to investigate the magnetic state of cerium atoms as a function of their environment.

References

1 I. Mayer and Y. Eshdat, *Inorg. Chem., 7* (1968) 1904.
2 E. I. Gladyshevsky, Crystal Chemistry of Silicides and Germanides, *Metallurgya,* 1971.
3 E. Houssay, A. Rouault, O. Thomas, R. Madar and J. P. Sénateur, *Appl. Surf. Sci., 38* (1989) 156.
4 H. Yashima, N. Sato, H. Mori and T. Satoh, *Solid State Commun., 43* (1982) 595.
5 H. Yashima, H. Mori, T. Satoh and K. Kohn, *Solid State Commun., 43* (1982) 193.
6 N. Sato, H. Mori, T. Satoh, T. Miura and H. Takei, *J. Phys. Soc. Jpn., 57* (1988) 1384.
7 H. Yashima, C. F. Lin, T. Satoh, H. Hiroyoshi and K. Kohn, *Solid State Commun., 57* (1986) 793.
8 R. Lahiouel, R. M. Galera, J. Pierre and E. Siaud, *J. Magn. Magn. Mater., 63-64* (1987) 98.
9 R. Madar, B. Lambert, E. Houssay, C. Meneau d'Anterroches, J. Pierre, O. Laborde, J. L. Soubeyroux, A. Rouault, J. Pelissier and J. P. Sénateur, *J. Mater. Res., 5* (1990) 2126.
10 B. Lambert-Andron, E. Houssay, R. Madar, F. Hippert, J. Pierre and S. Auffret, *J. Less-Common Met., 167* (1990) 53.
11 P. Schobinger-Papamantellos, T. Janssen, D. B. de Mooij and K. H. J. Buschow, *J. Less-Common Met., 162* (1990) 197.
P. Schobinger-Papamantellos, K. H. J. Buschow and T. Janssen, *Phase Transitions, 33* (1991) 133.

12 S. Auffret, J. Pierre, B. Lambert-Andron, R. Madar, E. Houssay, D. Schmitt and E. Siaud, *Physica B, 173* (1991) 265.
13 S. K. Dhar, K. A. Gschneidner, W. H. Lee, P. Klavins and R. N. Shelton, *Phys. Rev. B, 36* (1987) 341.
W. H. Lee, R. N. Shelton, S. K. Dhar and K. A. Gschneidner, *Phys. Rev., 16* (1987) 8523.
14 O. Thomas, J. P. Sénateur, R. Madar, O. Laborde and E. Rosencher, *Solid State Commun., 55* (1985) 629.
15 W. H. Dijkman, A. C. Moleman, E. Kesseler, F. R. de Boer and P. F. de Chatel, in P. Wachter and H. Boppart (eds.), *Valence Instabilities*, North Holland, Amsterdam, 1982, p. 515.
B. Lambert-Andron, F. Sayetat, S. Auffret, J. Pierre and R. Madar, *J. Phys. Condensed Matter, 3* (1991) 3113.
16 B. A. Frenz, *SPD Program*, College Station, Texas, 1985.
17 J. Pierre, O. Laborde, E. Houssay, A. Rouault, J. P. Sénateur and R. Madar, *J. Phys. Condensed Matter, 2* (1990) 431.